

Observation of an Atomic Stark–Electric-Quadrupole Interference

L. R. Hunter, W. A. Walker, and D. S. Weiss

Physics Department, Amherst College, Amherst, Massachusetts 01002

(Received 23 December 1985)

An interference between electric-quadrupole and Stark-induced dipole amplitudes is observed for the first time. Measurement of this interference in atomic strontium permits the first experimental determination of the decay rate between the lowest 1P and metastable 1D levels in an alkaline-earth atom. We obtain the result $A(5s5p-5s4d) = (3.85 \pm 0.94 \pm 0.53) \times 10^3 \text{ s}^{-1}$.

PACS numbers: 32.60.+i, 32.70.Cs, 35.80.+s

Stark-interference techniques provide powerful tools for the investigation of weak atomic transition amplitudes. Highly forbidden magnetic-dipole amplitudes in cesium and thallium have been successfully determined by use of Stark–magnetic-dipole interferences.^{1,2} Recently, atomic parity nonconservation due to neutral weak currents has been observed with use of Stark-interference methods.^{3–5} Theoretically, interference between the Stark and electric-quadrupole amplitudes results in a polarization of the excited atomic state in a direction orthogonal to both the propagation direction of the exciting radiation and the applied electric field. By use of this interference term, it is possible to measure the relative strengths of the Stark and electric-quadrupole amplitudes even on transitions where the quadratic Stark effect is unobservably small.

We report here the first observation of an interference between Stark and electric-quadrupole amplitudes in an atom. Our measurements have been carried out on the $(5s^2)^1S - (5s, 4d)^1D$ transition in strontium. By

observing the interference on this transition we are able to determine the transition rate from the lowest 1P state to the metastable 1D states of strontium. Present theoretical values for this decay rate differ by over 2 orders of magnitude as a result of a near cancellation between different electronic configurations.^{6–8} This decay is critical in the determination of the feasibility of the laser cooling of Sr. In addition, it is of interest in studies of energy pooling and two-photon and anti-Stokes lasers. While upper limits on the decay rates from the lowest 1P to the metastable 1D state have been previously reported in barium⁹ and calcium,¹⁰ the present work represents the first actual measurement of such a decay rate in the alkaline-earth series.

The $(5s^2)^1S - (5s, 4d)^1D$ transition is excited by a 496-nm laser, propagating along \hat{x} . The excitation occurs in the presence of an electric field (F) along \hat{y} that modifies the original eigenstates of the unperturbed Hamiltonian:

$$|4\tilde{D}\rangle = |4D\rangle + \sum_{\xi = ^1P \text{ and } ^1F \text{ states}} \frac{\langle \xi | eFY | 4D \rangle}{E_D - E_\xi} |\xi\rangle, \quad |5\tilde{S}\rangle = |5S\rangle + \sum_{^1P \text{ states}} \frac{\langle nP | eFY | 5S \rangle}{E_S - E_{nP}} |nP\rangle.$$

In the above expression the operator Y is the sum of the y coordinates of the atomic electrons, while E_n represents the energy of the n th eigenstate. The amplitude of an electromagnetic transition matrix element (EM) connecting the perturbed $5\tilde{S}$ and $4\tilde{D}$ states will then have an electric-dipole ($E1$) amplitude in addition to the usual electric-quadrupole ($E2$) amplitude:

$$\langle 4\tilde{D} | \text{EM} | 5\tilde{S} \rangle = \langle 4D | E2 | 5S \rangle + eF \sum_{nP} \frac{\langle 4D | Y | nP \rangle \langle nP | E1 | 5S \rangle}{E_D - E_{nP}} + \frac{\langle 4D | E1 | nP \rangle \langle nP | Y | 5S \rangle}{E_S - E_{nP}}.$$

The two dipole and the quadrupole transition matrices here may be written respectively as

$$\begin{aligned} & im\omega_{nPS} \langle n^1P | \mathbf{x}_j | ^1S \rangle \cdot \hat{\epsilon}, \\ & - im\omega_{nPD} \sum_j \langle ^1D | \mathbf{x}_j | n^1P \rangle \cdot \hat{\epsilon}, \\ & \frac{1}{2} m\omega_{DS} \mathbf{k} \cdot \sum_j \langle ^1D | \mathbf{x}_j \mathbf{x}_j | ^1S \rangle \cdot \hat{\epsilon}, \end{aligned}$$

where \mathbf{x}_j is the coordinate of the j th electron, ω_{ab} is the angular transition frequency between the states a and b , and \mathbf{k} and $\hat{\epsilon}$ are the propagation and polarization

vectors associated with the 496-nm radiation. Solving the angular integrals yields the relative transition probabilities to the various magnetic sublevels of the 1D state shown in Fig. 1. The quantities S and Q represent respectively the Stark-induced dipole and the electric-quadrupole transition amplitudes and are given by

$$S = -\frac{meF}{\hbar\sqrt{30}} \sum_{nP} \left(\frac{\omega_{nPD}}{\omega_{nPS}} - \frac{\omega_{nPS}}{\omega_{nPD}} \right) R_{nPD} R_{nPS}$$

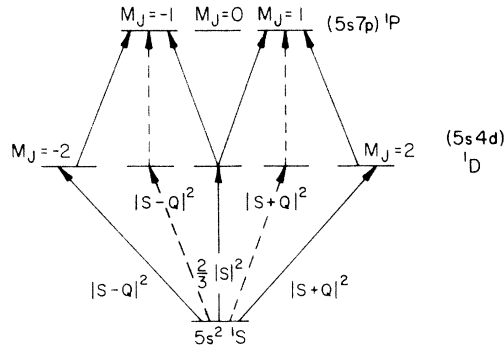


FIG. 1. Relative excitation probabilities for the various magnetic sublevels. S and Q represent the Stark and quadrupole amplitudes. The solid (dashed) lines are the transitions for the two beams polarized along \hat{y} (\hat{z}).

and

$$Q = -m\omega_{DS}^2 R_{DS} / 2c\sqrt{30},$$

where the R_{ab} is the relevant radial integral between the states a and b . The energy separation between the $5P$ and $4D$ levels in strontium is particularly small ($\approx 1550 \text{ cm}^{-1}$), so that the infinite sum for S is dominated by the mixing of the $5P$ level. Upon examination of Fig. 1 it is evident that the interference terms between the Stark and electric-quadrupole amplitudes cancel in the total intensity. The interference does, however, result in a polarization of the $1D$ state along z : $P_I = KQS^*/|Q|^2$, where we have assumed $|S|^2 \ll |Q|^2$ and have introduced the parameter K that has the value 1 for ϵ along z and 2 for ϵ along y . To analyze P_I , the $1D$ state is excited to the $(5s, 7p) 1P$ level with a 533-nm laser, propagating along $-\hat{x}$ and linearly polarized parallel to the polarization of the 496-nm laser. The resulting polarization of the $1P$ level (see Fig. 1) is analyzed by examination of the circular polarization of its decay fluorescence at 533 nm.

A schematic of the apparatus used is shown in Fig. 2. The experiment is performed in a stainless-steel cross cell with about 0.1 Torr of helium present to keep the windows from coating with Sr. The Sr density is about 10^{-14} cm^{-3} . Three pairs of rectangular magnetic field coils are used to cancel the Earth's field and to apply external magnetic fields for calibration and diagnostics. The stainless-steel electrode structure has been designed to minimize discharges and scattered-light backgrounds. The spacing between the parallel electrodes is 6.94 mm at our operating temperature. High voltage is applied across these electrodes in 1- μs pulses in order to minimize discharge effects and the resulting screening of the field.

A flashlamp-pumped dye laser excites the 496-nm transition. The 1-mJ, 0.5- μs laser pulse is carefully overlapped with the electric field pulse. Approximate-

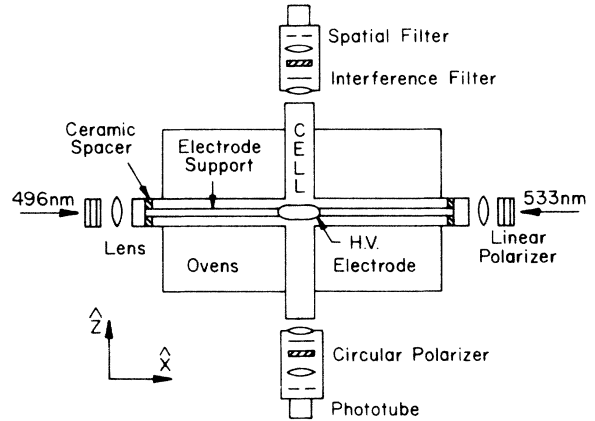


FIG. 2. Experimental apparatus. The high-voltage electrode is centered in the cell. A flat electrode held at $V = 0$ (not shown) rests on the cell floor.

ly 20 mW of 533-nm radiation is generated by an argon-ion-pumped dye laser. Two phototubes, oriented along the $\pm \hat{z}$ axis and equipped with identical circular polarization analyzers and interference filters, detect the 533-nm decay fluorescence from the $1P$ state. The integrated current from these phototubes is digitized and stored after each laser pulse. The difference of the phototube signals divided by their sum yields an asymmetry (η) that is proportional to the polarization of the $1D$ level, and is independent of the laser intensity and frequency fluctuations.

In order to determine the linear coefficient that relates the observed asymmetry to the atomic polarization, a known polarization must be created along \hat{z} . This calibration polarization is produced by replacing the electric field by a magnetic field (\mathbf{B}) along \hat{z} and tuning the 496-nm laser to the side of the atomic resonance. The preferential absorption by the magnetic sublevels Zeeman shifted towards line center results in a polarization of the $1D$ state: $P_c = 4K^2 \ln 2 \Delta\gamma \gamma_z / \gamma_a^2$. Here $\gamma_z = \mu_0 B / h$ is the Zeeman splitting of the $1D$ state, γ_a is the FWHM of the Gaussian absorption profile, and $\Delta\gamma$ is the laser detuning from line center. The expression for P_c assumes that $\gamma_z \ll \gamma_a$. The magnitude of $\Delta\gamma$ is equal to $\frac{1}{2} \gamma_a [\ln(r) / \ln(2)]^{1/2}$, where r is the ratio of the absorption intensity at line center to the intensity observed on the side of the line. γ_a is determined through the equation $\gamma_a = [(\gamma_D)^2 + (\gamma_l)^2]^{1/2}$, where γ_D and γ_l are respectively the Doppler and laser widths. γ_D is determined from the measured cell temperature to be 1.34 GHz. The laser profile is observed by means of a Fabry-Perot etalon and found to be approximately Gaussian with a width of $750 \pm 100 \text{ MHz}$. The resulting absorption width has also been measured directly and is found to agree quite well with the predicted width. The effect of the optical

isotope shift on P_c was considered and found to be insignificant.

Data are collected by summing the integrated phototube voltages over ten laser pulses and constructing the asymmetry η . The electric field is then reversed and the asymmetry is constructed from the signals averaged over the next ten laser pulses. Since P_l changes sign with the reversal of F , the average difference of these asymmetries $\bar{\eta}$ is formed.

The normalization data are collected in an identical manner except that (1) the reversing electric field is now replaced by a reversing magnetic field along \hat{z} with a magnitude of 18.9 ± 0.1 G; and (2) the 496-nm laser is tuned to the side of the absorption profile so that $r \approx 4$. Because the normalization asymmetry reverses with the sign of $\Delta\gamma$, the average difference is taken between alternate data sets, collected with the laser detuned to opposite sides of the line profile. Between each data set the magnitude of the signal at line center is measured so that r and the magnitude of $\Delta\gamma$ may be precisely determined.

With the analyzing laser polarized along \hat{y} and a magnetic field along \hat{z} , the excitation frequencies associated with the analyzing transition are different for the various magnetic sublevels. If the frequency of the analyzing laser drifts to either side of line center, polarizations are induced in the $7P$ level. To avoid this potential systematic error, only data with the laser polarizations aligned along \hat{z} are included in our analysis.

A total of four days of data are included in our final data set: two with \mathbf{k} along \hat{x} and two with \mathbf{k} along $-\hat{x}$. The electric-quadrupole amplitude changes sign with the reversal of \mathbf{k} , resulting in a sign change in P_l . If this sign change is accounted for, the normalized data from these four days agree very well and may be combined. The results are shown in Fig. 3. While the data are reasonably well fitted by a straight line, there appears to be some deviation from linearity at the highest voltages. We believe this deviation to be due to partial shielding of the applied field at these voltages by space charge. These charges are probably liberated by the weak, pulsed glow discharge which is observed at high voltage. The slopes (s) and intercepts (i) associated with the best-fit lines found when successive high-voltage points are eliminated are, in units of percent per kilovolt and percent, respectively, 0–500 V, $s = 2.07 \pm 0.08$, $i = 0.38 \pm 0.10$; 0–400 V, $s = 2.22 \pm 0.10$, $i = 0.22 \pm 0.19$; 0–300 V, $s = 2.46 \pm 0.14$, $i = 0.00 \pm 0.21$; and 0–200 V, $s = 2.46 \pm 0.20$, $i = 0.01 \pm 0.24$. Since the zero-voltage point corresponds to a difference being taken between two identical geometries, we expect that the correct line must pass through the origin. On the basis of these considerations we have decided to exclude the 400- and 500-V data from our analysis. The slopes analyzed separately for \mathbf{k} along $+\hat{x}$ and $-\hat{x}$ are respectively 2.62 ± 0.23

and -2.37 ± 0.18 , clearly exhibiting the anticipated change of sign. With inclusion of the uncertainty associated with the laser width, our results imply that at $F = 1$ kV/cm, $S/Q = (1.71 \pm 0.11)\%$. The observed polarization is in the $+\hat{z}$ direction when F is along \hat{y} and \mathbf{k} is along \hat{x} .

To deduce the spontaneous decay rate $A(5s5p^1P-5s4d^1D)$ from our measured polarization we require the radial matrix elements R_{SP} and R_{SD} . These are obtained from the transition rates through the expressions

$$\begin{aligned} A(5s5p^1P-5s5s^1S) &= \frac{4}{9} \alpha \omega_{SP}^3 R_{SP}^2 / c^2 \\ &= (2.04 \pm 0.05) \times 10^8 \text{ s}^{-1} \end{aligned}$$

(experimental summary in Ref. 7) and

$$A(5s4d^1D-5s5s^1S) = \frac{1}{75} \alpha \omega_{SD}^5 R_{SD}^2 / c^4 = 44.7 \text{ s}^{-1}$$

(Ref. 8). In view of the excellent agreement between theory⁸ and experiment¹¹ on the comparable quadrupole transition in calcium, we assume that the predicted quadrupole decay rate is in error by no more than 20%. Using these values, our results, the expressions for Q and S , and the equation $A(5s5p^1P-5s4d^1D) = \frac{8}{9} \alpha \omega_{PD}^3 R_{DP}^2 / c^2$ and assuming that our entire polarization is due to the mixing of the 5^1P level, we find

$$\begin{aligned} A(5s5p^1P-5s4d^1D) \\ = (3.85 \pm 0.94 \pm 0.53) \times 10^3 \text{ s}^{-1}. \end{aligned}$$

The first uncertainty represents the combined one-standard-deviation statistical uncertainty and the second represents the maximum modification of our result that could be expected from the Stark interference associated with all the other 1P levels. In order to

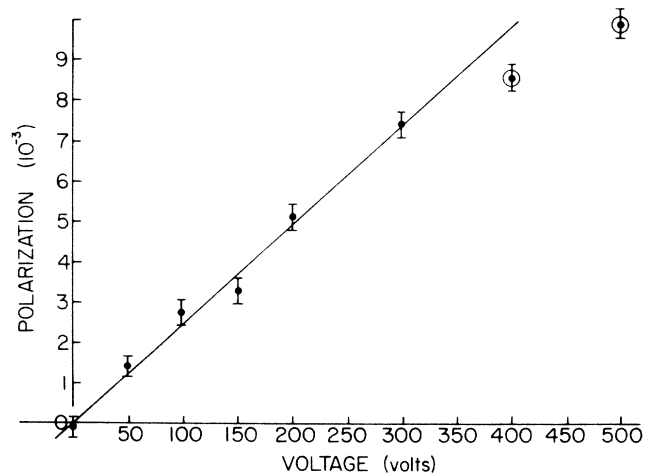


FIG. 3. The normalized polarization of the 1D state as a function of applied voltage. The two circled points have not been included in the linear fit shown.

TABLE I. Theoretical values for $A(5s5p\ ^1P-5s4d\ ^1D)$ in strontium. MC = multiconfiguration, HF = Hartree-Fock, l = length representation, and v = velocity representation.

Reference	Method	Result (s^{-1})
a	Semiempirical	1.1×10^5
b	HF/ l	4.8×10^4
b	HF v	1.0×10^4
b	MC HF/ l	2770
b	MC HF v	800
c	Relativistic with core valence correlations	1344

^aReference 6.

^cReference 8.

^bReference 7.

arrive at this latter number we use the oscillator-strength measurements of Parkinson, Reeves, and Tomkins¹² to determine the magnitude of $A(5snp\ ^1P-5s5s\ ^1S)$ and the corresponding R_{SnP} for $5 < n < 22$. Using the n^1P lifetime measurements of Jonsson *et al.*¹³ we place an upper limit on $A(5snp\ ^1P-5s4d\ ^1D)$ and the corresponding R_{nPD} by making the conservative assumption that the decays to the ground and metastable states together account for the total observed lifetimes. The contributions of the states with $n > 21$ are calculated by taking the observed rates for high n and assuming that they continue to fall off with the anticipated $1/n^3$ dependence. The infinite sum is easily calculated and found to produce only a small effect. In arriving at this upper limit we also make the conservative assumption that the signs of all the contributing terms are the same, but allow that this sign be either the same as or opposite to that of the dominant term of interest.

In Table I we list the previous theoretical estimates of this decay rate. It is evident that our result represents a vast improvement over the previous

knowledge of this important decay rate. We now hope to use this technique to measure the comparable transition rates in Ca and Ba.

We thank J. Guena for reading our original calculations; E. D. Commins, W. L. Lichten, and A. G. Zajonc for equipment loans; and Digital Equipment Corp. for the donation of our data acquisition system. This research was supported by grants from Research Corporation, the Hewlett Foundation, the National Science Foundation, and the National Bureau of Standards. Acknowledgment is also made of the special research funds made available for this project by Amherst College.

¹S. Chu, E. D. Commins, and R. Conti, Phys. Lett. **60A**, 96 (1977).

²M. A. Bouchiat, J. Guena, and L. Pottier, J. Phys. (Paris), Lett. **45**, L61 (1984).

³P. Bucksbaum, E. D. Commins, and L. Hunter, Phys. Rev. Lett. **46**, 640 (1981); P. S. Drell and E. D. Commins, Phys. Rev. Lett. **53**, 968 (1984).

⁴M. A. Bouchiat, J. Guena, L. Hunter, and L. Pottier, Phys. Lett. **117B**, 358 (1982); and **134B**, 463 (1984).

⁵S. L. Gilbert, M. C. Noecker, R. N. Watts, and C. E. Wieman, Phys. Rev. Lett. **55**, 2680 (1985).

⁶V. A. Zilitis, Opt. Spectrosc. (Engl. Transl.) **29**, 438 (1970).

⁷J. E. Hansen, J. Phys. B **11**, L579 (1978).

⁸C. W. Bauschlicher, S. R. Langhoff, and H. Partridge, J. Phys. B **18**, 1523 (1985).

⁹A. F. Bernhardt, D. E. Duerre, J. R. Simpson, and L. L. Wood, J. Opt. Soc. Am. **66**, 416 (1976).

¹⁰S. K. Peck and L. R. Hunter, Opt. Commun. **54**, 12 (1985).

¹¹K. Fukuda and K. Ueda, J. Phys. Chem. **86**, 676 (1982).

¹²W. H. Parkinson, E. M. Reeves, and F. S. Tomkins, J. Phys. B **9**, 157 (1976).

¹³G. Jonsson, C. Levinson, A. Persson, and C.-G. Wahlstrom, Z. Phys. A **316**, 255 (1984).